Knee Flexion-Assisted Method for Human-Exoskeleton System

Zhipeng Wang, Chifu Yang, Shengping Zhang, *Member, IEEE*, Shihao Zhang, Chunzhi Yi, *Member, IEEE*, Zhen Ding, Baichun Wei, and Feng Jiang, *Member, IEEE*

***Abstract*— The knee has gradually become an important research target for the lower extremity exoskeleton. However, the issue that whether the flexion-assisted profile based on the contractile element (CE) is effective throughout the gait is still a research gap. In this study, we first analyze the effective flexion-assisted method through the passive element's (PE) energy storage and release mechanism. Specifically, ensuring assisting within an entire joint power period and the human's active movement is a prerequisite for the CE-based flexion-assisted method. Second, we design the enhanced adaptive oscillator (EAO) to ensure the human's active movement and the integrity of the assistance profile. Third, a fundamental frequency estimation based on discrete Fourier transform (DFT) is proposed to shorten the convergence time of EAO significantly. The finite state machine (FSM) is designed to improve the stability and practicality of EAO. Finally, we demonstrate the effectiveness of the prerequisite condition for the CE-based flexion-assisted method by using electromyography (EMG) and metabolic indicators in experiments. In particular, for the knee joint, CE-based flexion assistance should be within an entire joint power period rather than just in the negative power phase. Ensuring the human's active movement will also significantly reduce the activation of antagonistic muscles. This study will aid in designing assistive methods from the perspective of natural human actuation and apply the EAO to the human-exoskeleton system.**

Manuscript received 4 May 2023; revised 9 June 2023; accepted 16 June 2023. Date of publication 20 June 2023; date of current version 28 June 2023. This work was supported in part by the National Natural Science Foundation of China under Grant 62076080, in part by the Natural Science Foundation of Chong Qing under Grant CSTB2022NSCQ-MSX0922, and in part by the Postdoctoral Science Foundation of Heilongjiang Province of China under Grant LBH-Z22175. *(Corresponding authors: Feng Jiang; Chunzhi Yi.)*

This work involved human subjects or animals in its research. Approval of all ethical and experimental procedures and protocols was granted by the Chinese Ethics Committee of Registering Clinical Trials under Application No. ChiECRCT20200319, and performed in line with the Declaration of Helsinki.

Zhipeng Wang, Chifu Yang, Shihao Zhang, and Zhen Ding are with the School of Mechatronics Engineering, Harbin Institute of Technology, Harbin, Heilongjiang 150001, China (e-mail: 19B908078@stu.hit.edu.cn; cfyang@hit.edu.cn; 21S008029@hit.edu.cn; 16b908060@stu.hit.edu.cn).

Shengping Zhang is with the School of Computer Science and Technology, Harbin Institute of Technology, Weihai, Shandong 264209, China (e-mail: s.zhang@hit.edu.cn).

Chunzhi Yi, Baichun Wei, and Feng Jiang are with the Faculty of Computing and the School of Medicine and Health, Harbin Institute of Technology, Harbin, Heilongjiang 150001, China (e-mail: chunzhiyi@hit.edu.cn; 18B903018@stu.hit.edu.cn; fjiang@hit.edu.cn).

Digital Object Identifier 10.1109/TNSRE.2023.3287867

***Index Terms*— Knee flexion-assisted method, energy storage and release mechanism, enhanced adaptive oscillator, human-exoskeleton system.**

I. Introduction

RESEARCH on the knee exoskeleton has gradually developed in recent years [1], [2], [3], [4]. The knee exoskeleton can be used for patient rehabilitation training [5], [6], [7] and the motion enhancement [8], [9], [10] of healthy individuals. Wearable, flexible exoskeletons [11], [12] have been widely used to assist healthy individuals due to their high integration and flexible movement advantages. The power source of the knee is its associated mono- and bi-articular muscles [13]. The challenge of designing a knee exoskeleton comes not only from structure and control methods [8], [9]. The complexity of multi-muscle-tendon units' coordinated movements [14], [15], [16] also poses a challenge for exoskeleton assistance.

Some studies have developed assistance profiles based on surface EMG signals [17], [18], [19]. Assistance methods based on proportional EMG [20] and mechanical measurements are compared. The test results show that there is no significant difference in metabolic reduction. However, muscle activation is higher based on the proportional EMG control. The test results suggest that neural control is more suitable for rehabilitation training. In [17], the assistance profile is obtained through the neuromuscular model. A variable stiffness profile [18] is also proposed based on the skeletal-muscle model. The experimental results in the abovementioned studies demonstrate that assistance based on the neuromuscular model can reduce muscle activation. However, physiological differences between participants and muscle fatigue increase the experimental workload and the difficulty of model calibration. In [21], the assistance profiles based on biomechanics, impedance control and proportional EMG are compared. The metabolic reduction under the three conditions is nearly identical, which is in line with the conclusion obtained in [20]. In contrast, participants prefer a biomechanical or impedance-controlled assistance profile. Currently, assistance profiles based on biomechanics are more used for ankle and hip joints [12], [22], [23].

Other than the shape of the assistance profile, accurate timing is also necessary for effective assistance. The assistance profile [24] is a function of the gait percentage. Usually, the

gait cycle is not a constant value. Therefore, the phase division method based on the previous gaits [25] is challenging to ensure the integrity of the assistance profile in the current gait. The adaptive oscillator (AO) [26], [27] is proposed to estimate the gait phase in previous research. However, the learning time of AO is usually 2.5-3.5 minutes and even longer. During the learning process, the output signal of AO is random. It cannot be used to divide the gait or compensate for the motion, limiting the practicality of AO in exoskeleton assistance.

Regarding high-efficiency energy utilization, studies suggest that the muscle-tendon unit's PE should be thoroughly evaluated during walking [28], [29], [30]. In [31], the proportion of PE in the biological moment of the knee is significantly higher than that in the ankle and hip joints. Previous studies have shown that the metabolism is primarily produced by the muscle-tendon unit's CE [32], [33]. Therefore, the lower energy consumption of the knee joint may be due to its more efficient energy storage and release mechanism [34]. The flexion assistance based on CE [35] is designed at terminal swing. Whether the CE-based knee flexion-assisted method can be further optimized in other gait phases has yet to be further studied [35], [36], [37]. Therefore, this paper will analyze and detect the effectiveness of the CE-based knee flexion-assisted method throughout the gait, which has a guiding role in understanding exoskeleton assistance and further research.

In that context, we develop an effective knee flexion-assisted method based on the PE's energy storage and release mechanism. The partial torque generated by CE is replaced by the assistance torque under the premise of ensuring assisting within an entire joint power period and the human's active movement. The gait phase division and angle prediction are designed based on EAO to ensure the integrity of the assistance profile within each gait cycle and the human's active movement. To enhance the practicality of the EAO in the human-exoskeleton system, we developed the fundamental frequency estimation method based on DFT and FSM. Finally, experiments demonstrate the effectiveness of the prerequisite condition for assistance. Our contributions can be summarized as follows.

1) To the best of our knowledge, we, for the first time, analyze and detect the effectiveness of the CE-based knee flexion-assisted method throughout the gait from the perspective of natural human actuation.

2) We demonstrate that assisting within an entire joint power period and the human's active movement is not disturbed is a prerequisite for effective the CE-based knee flexion-assisted method.

3) We demonstrate that the proposed DFT and FSM can significantly shorten the convergence time and enhance the stability and practicality of the EAO in the human-exoskeleton system.

This paper is organized as follows. Section II analyzes and derives the effective assistance method. Section III describes the corresponding control methods. The experimental results are presented and discussed in Section IV and Section V. The conclusion is given in Section VI.

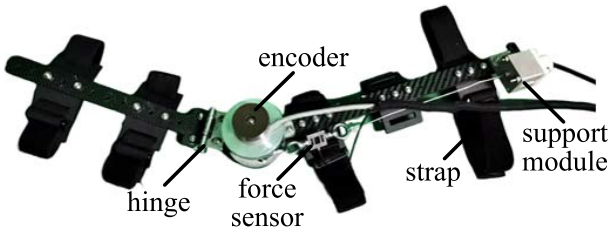

Fig. 1. The fixation mechanism of the knee joint.

II. Assistance Methods

A. Exoskeleton

A wearable exoskeleton with Bowden cable as the transmission is introduced in this paper. The knee exoskeleton consists of a power unit and a fixation mechanism. The power unit is integrated near the center of body weight to reduce extra metabolic consumption. The fixation mechanism of the knee joint shown in Fig. 1 is designed considering the advantages of easy sensor installation (for detailed specifications, see [38]). Two carbon fiber plates and a hinge form a rotational joint in the sagittal and coronal planes of the knee joint, respectively. Compared to the previous version, the baffle is replaced by straps to facilitate the measurement of EMG signals. The straps counteract the internal force generated by the inner cable in the vertical direction of the lower limbs. On the other hand, the sliding of the fixation mechanism along the direction of the lower limbs is limited by a strap connected to the waist belt. The weight of the fixation mechanism is 0.7kg. The knee exoskeleton presented in this paper is applied to enhance the sport's ability of healthy individuals.

B. Flexion-Assisted Analysis Based on PE

The knee joint connects the femur and tibia. Muscle groups are composed of flexor and antagonist muscles in parallel. The knee biological moment is generated through the CE and PE of all muscles. The force generated by CE depends on joint angle and muscle activation [39]. The contraction of CE is accompanied by energy consumption. The PE can be equivalent to a nonlinear spring, as shown follows

$$F_P^m = f_P(l) F_0^m \tag{1}$$

$$f_P(l) = e^{10l-15} \tag{2}$$

$$l = l^m / (l_0^m (\lambda(1 - a(k)) + 1)) \tag{3}$$

where F_P^m is the force generated by PE; $f_P(l)$ is the force-length relationship of PE; F_0^m is the maximum isometric muscle force; l is the normalized muscle fiber length; l^m is the length of muscle fiber; l_0^m is the optimal fiber length; λ is constant; $a(k)$ is the muscle activation.

The PE equation is written to gain a clearer understanding of PE's role in the knee joint's net moment. Energy is stored in the elastic element when the PE and tendon are elongated during the negative work phase. In the positive work phase, the stored energy is rereleased with the contraction of CE. PE's energy storage and release mechanism is a chain reaction after the action of CE.

It can be seen from (1)-(3) that the stored energy in PE decreases as muscle activation decreases during the negative

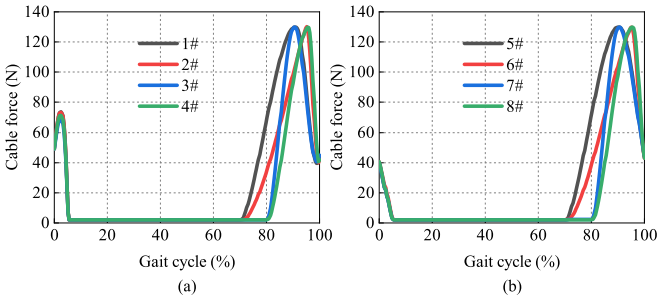

Fig. 2. Designed assistance profiles based on joint power period.

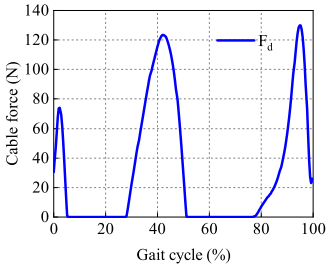

Fig. 3. Preliminary knee flexion-assisted profile.

work phase. If the assistance is not sustained during the positive work phase, CE may need to increase to compensate for the energy lost by PE during the negative work phase.

On the other hand, the knee joint's motion changes will affect each joint's mechanical balance, the length of muscle fibers and PE's energy storage and release mechanism. To ensure that the energy feedback mechanism is not disturbed, the joint motion should not be significantly altered due to the intervention of the exoskeleton. In other words, assistance should be based on not hindering the human's active movement.

A set of experiments is first conducted independently to verify the necessity of assisting within an entire joint power period and human's active movement. Compared with the terminal stance, the demarcation between negative work and positive work is more significant in the terminal swing and initial contact. Therefore, we first design a set of comparative experiments to verify the necessity of continuous assistance in the terminal swing and initial contact. At terminal swing, the flexion moment's onset timing is between 70% and 80% of the gait cycle, while the flexion moment's peak timing is between 90% and 95% [40]. We design four different assistive curves shown in Fig. 2(a) within the statistical range to reduce the influence of assist timing. Simulating human torque has been used and proven effective in ankle joints [41], [42]. Additional unimodal curves shown in Fig. 2(b) are added as comparative experiments to demonstrate the effectiveness of assisting within an entire power period. Discrete points are first defined within the statistical range of the joint torque curves. The assistance profiles were then fitted by the cubic spline method. The experiment is completed 2 times. The random 2 sets of profiles in Fig. 2(a) and the corresponding unimodal profiles in Fig. 2(b) are selected in the first experiment. The remaining profiles are selected in the second experiment. The interval between experiments is 2 days. First, a 6-min standing test is performed to test their basal metabolism. Participants then rest for 5 minutes. When the experiment starts, the participants walk without assistance for 6 minutes and then walk with assistance in random order. Each assist mode lasts 6 minutes, with a 5-minute rest period between assistance modes.

The net moment of the knee joint at the terminal swing, initial contact and terminal stance all show flexion moments. A preliminary assistance method for the knee is obtained through the above analysis. The following content needs to be considered. First, the partial torque generated by CE is replaced by the assistance torque under the premise of not affecting the human's active movement and the PE's energy storage and release mechanism. Therefore, the assistance profile equivalent to the Bowden cable is preliminarily obtained by subtracting the torque generated by PE [31] from the net biological moment [38], [40], as shown in Fig. 3. Second, the assistance profile is a function of the gait percentage (0-100%). Even if the gait cycle is not a constant value, the assistance profile within a gait cycle should be complete and continuous.

III. Control Architecture

A. EAO Design Based on DFT and FSM

The joint angle during walking can be regarded as a periodic signal. The parallel EAOs can learn the frequency and phase changes of the joint angle. The gait is not entirely consistent. Therefore, the natural frequency and output value of EAO are set as a state variable, as shown below

$$\dot{\phi}_i(t) = i\omega(t) + v_1(\theta_h(t) - \hat{\theta}_h(t)) \tag{4}$$

$$\dot{\omega}(t) = v_1(\theta_h(t) - \hat{\theta}_h(t))\cos(\phi_1(t)) \tag{5}$$

$$\hat{\theta}_h(t) = \sum_{i=1}^{j} \alpha_i(t)\sin(\phi_i(t)) + \alpha_0(t) \tag{6}$$

$$\dot{\alpha}_i(t) = \eta(\theta_h(t) - \hat{\theta}_h(t))\sin(\phi_i(t)) \tag{7}$$

where $\phi_i(t)$ is the phase of the i-th EAO; $\omega(t)$ is the EAO's fundamental frequency; v_1 is the proportional coefficient; $\theta_h(t)$ is the response value of EAO; $\alpha_i(t)$ is the amplitude of the output signal of the i-th EAO; and η is the integral gain.

To improve the convergence speed of EAO, the joint angle data for the 5 s time window are collected and preprocessed by (8). The design method of EAO is slightly different for control units with different sampling periods. Specifically, k and P in (8) depend on the cycle periods of the corresponding control unit.

$$X(k) = \sum_{i=0}^{P-1} x(i)e^{-j2\pi\frac{k}{N}i} \quad k = 0, 1, \cdots, P-1 \tag{8}$$

where $P = 5fs$, fs is the sampling frequency of the joint angle, $fs = 250$ Hz; and $x(i)$ is sampled value of the i-th joint angle in the time window.

The frequency corresponding to $X(k)$ is shown in (9).

$$f_k = k(fs/P) \tag{9}$$

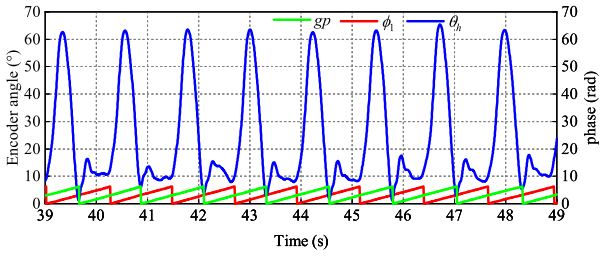

Fig. 4. Gait segmentation curve based on phase.

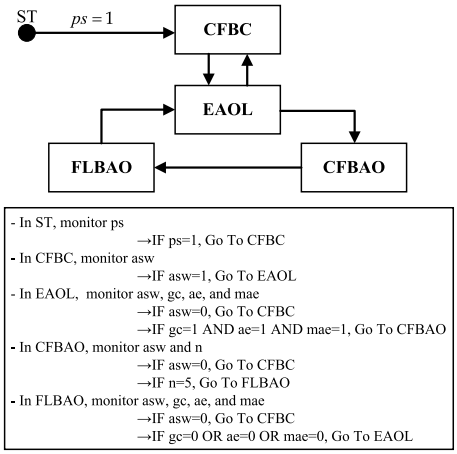

Fig. 5. Control block diagram of FSM.

The initial value of the fundamental frequency $\omega(0)$ is obtained when (10) is satisfied for the first time.

$$|X(k+2)| - |X(k+1)| > 20(|X(k+1)| - |X(k)|) \quad (10)$$

$$\omega(0) = 2\pi f_{k+2} \quad (11)$$

The gait segmentation curve based on ϕ_1 is shown in Fig. 4. However, ϕ_1 does not coincide with the initial landing when $\phi_1 = 0$. Therefore, the phase offset is introduced into the calculated gait percentage. The corresponding phase offset is a constant value, which is also the advantage of EAO in estimating the gait phase. The gait percentage obtained based on EAO is as follows

$$gp = \frac{(\phi_1 + os) \mod 2\pi}{2\pi} \quad (12)$$

where os is the phase offset, $os = 3.075$; and the mod is remainder operator.

The learning and switching of EAO are achieved based on FSM, shown in Fig. 5. First, the human stands (ST) and waits for the power switch (ps) to be turned on. Because of the high flexibility, the inner cable may not be tensioned before the experiment. When the power switch is turned on, the motor rotates at a speed of 0.3 r/min until a preload of 10 N. Subsequently, the constant-value force control mode (CFBC) is switched based on knee joint angle compensation. Second, when the assistance switch (asw) is turned on, the joint angle data for the 5 s time window are collected to calculate $\omega(0)$. The switch can be turned off to ensure the safety of participants in an emergency. Third, EAO learning (EAOL) is initiated. The average error (ae) between the predicted signal and the input signal in the 1.2 s time window, the gait cycle (gc) and the maximum error (mae) are all used as the judgment conditions for learning completion. When the learning of EAO is completed, the displacement compensation (CFBAO) is gradually switched to the predicted signal of the EAO output within five gait cycles. Fourth, the force command (FLBAO) is switched from a constant value to an assistance profile based on the gait cycle of EAO. When the EAO needs to be relearned, the control mode is switched to EAO learning.

B. Controller Design of Inner Loop and Outer Loop

The controller is discussed in detail to guarantee the force loading performance in our previous study [38]. The system control block diagram is shown in Fig. 6. First, a disturbance observer (DOB) is designed to compensate for the disturbance of the parameter perturbation and Bowden cable friction to the inner loop. In the outer loop, an admittance control is proposed. The feedforward model shown in (13) is designed to compensate for the elastic deformation of the human-exoskeleton interface. The iterative controller shown in (14) is proposed to compensate for the inelastic deformation of the human-exoskeleton interface and the displacement error caused by the speed loop.

$$\dot{\theta}_{ed} = \frac{nC_{fd1}C_{fd2}}{r_e(C_{fd2}F_d + 1)} \quad (13)$$

$$\dot{\theta}_{ci} = \begin{cases} \dfrac{0.0005}{T_{ei}} n\delta_i & \dfrac{e_{F_{i-1}}}{K} > 0.0005 \\ \dfrac{e_{F_{i-1}}}{KT_{ei}} n\delta_i & 0.0005 \geq \dfrac{e_{F_{i-1}}}{K} \geq -0.0005 \\ -\dfrac{0.0005}{T_{ei}} n\delta_i & -0.0005 > \dfrac{e_{F_{i-1}}}{K} \end{cases} \quad (14)$$

where n is the reduction ratio; C_{fd1} and C_{fd2} are the fitting coefficients, respectively; r_e is the radius of the sheave; F_d is the force command equivalent to the Bowden cable; δ_i is the speed correction coefficient; $e_{F_{i-1}}$ is the maximum force error of the previous gait cycle; K is the comprehensive stiffness of the transmission mechanism between the servo motor and the fixation mechanism; $\dot{\theta}_{ci}$ is the current gait speed correction value; and T_{ei} is the average value of the previous two gait cycles.

A kernel-based nonlinear filter is introduced based on (6) to predict the knee joint angle, effectively reducing additional antagonist muscle activation caused by disturbance force.

$$\hat{\theta}_{hf,\Delta_\phi}(t) = \frac{\sum \exp(h(\cos(\phi_1(t) + \Delta_\phi - c_i) - 1))\omega_i}{\sum \exp(h(\cos(\phi_1(t) + \Delta_\phi - c_i) - 1))} \quad (15)$$

where h is the width of the kernel function; $c_i = \frac{2\pi}{N}i$, N is the number of kernel functions; and ω_i is the weighting factor.

The compensation term for human motion is as follows

$$\dot{\theta}_{hf,\Delta_\phi}(t) = \frac{nr_h}{r_e} \frac{\mathrm{d}(\hat{\theta}_{hf,\Delta_\phi}(t) - \theta_{h1,\Delta}(t))}{\mathrm{d}t} \quad (16)$$

where r_h is the radius of the sheave at the knee joint. The fundamental frequency estimation method is developed based on DFT and FSM to enhance the practicality of the EAO in the human-exoskeleton system.

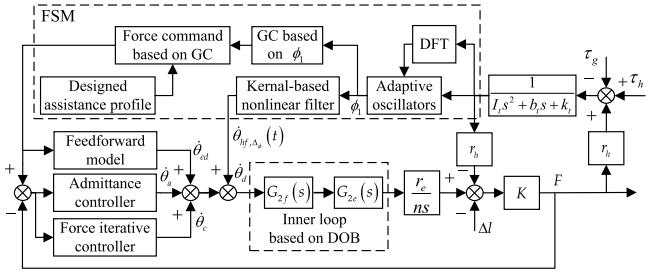

Fig. 6. Control block diagram of human-exoskeleton system.

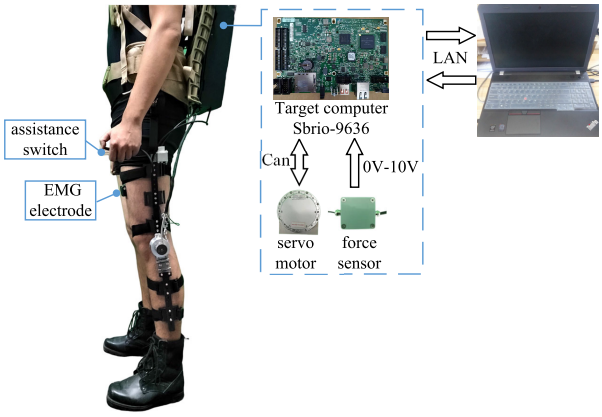

Fig. 7. The designed human-exoskeleton system.

IV. Experiment

A. Testing Protocol

Participants walk on a treadmill in 3 random sequences at 4.5 km/h. The modes are: 1) normal participant walking (NW) without the exoskeleton; 2) based on the traditional displacement compensation, the participant walking with the exoskeleton under zero force (ZF) command; 3) based on EAO, the participant walking with the exoskeleton under the assistance profile (AP). Experiments are performed consecutively. Before the experiment begins, participants stand for 10 minutes to test their basal metabolism. Each walking task lasts 10 minutes, with a 10-minute break after the test. The experimental data of 7.5-9.5 minutes are selected to ensure the adaptability of the participants under different tasks.

Human metabolic rates are measured using indirect calorimetry. The main method is to measure the participants' oxygen consumption and carbon dioxide production during exercise (COSMED, Italy). The rectus femoris (RF), vastus medialis (VM), semitendinosus (SEM), long head of biceps femoris (BF) and gastrocnemius (GAS) are selected to investigate the effect of assistance on bi-articular and antagonistic muscles. EMG signals are collected using a wireless surface EMG system (DELSYS, MA, USA). The EMG signal processing steps are as follows. First, the EMG signal is high-pass filtered at 20 Hz using a fourth-order zero-phase-shift Butterworth filter. Second, the signal is full-wave rectified. Finally, the signal is low-pass filtered at 6 Hz using a fourth-order zero-phase-shift Butterworth filter [43]. The amplitudes of the pre-processed EMG signals are normalized by the maximum under all assistance patterns. The root mean square (RMS) of the EMG signal is chosen as the primary indicator of muscle activity. One-way Analysis of Variance (ANOVA) is used to analyze whether muscle activities reduced significantly compared to NW. The significance level is set $\alpha = 0.05$. The designed human-exoskeleton system is shown in Fig. 7. Sbrio-9636 is adopted as the lower computer to improve the integration. The frequency of the control system is 250 Hz. Finally, we also separately test the effectiveness of the fast convergence of the EAO method at walking speeds of 4.5km/h, 5.5km/h, and 6.5km/h, respectively.

B. Participants

Seven healthy males are recruited to participate in this experiment (age $= 30 \pm 5$ years, mass $= 75 \pm 8$ kg, height $= 1.75 \pm 0.06$ m). All participants had walking experience wearing knee exoskeletons. All participants confirmed that there was no gait disturbance or injury. Informed consent for inclusion was given by each participant before participation in the study, which was conducted according to the Declaration of Helsinki. The study protocol of Registering Clinical Trials (ChiECRCT20200319) was approved by the Chinese Ethics Committee.

C. Results

The muscle activities and net metabolic rate under the designed eight assistance profiles are shown in Figs. 8 and 9, respectively. The energy consumption of assisting within an entire joint power period is lower than that of assisting only in the negative power phase. With the decrease of energy metabolism, muscle activity of the corresponding flexors and antagonists decreases. At the initial contact, the flexor and antagonistic muscles work together to withstand the impact of landing. Optimal flexion assistance can replace part of the role of antagonistic muscles, while reducing the muscle activation of flexor muscles and antagonistic muscles. Notably, there is also an increase in the antagonist's muscle and a decrease in the flexor muscle in Fig. 8. While energy consumption is reduced, it's not the best assistance mode. Experimental results verify that knee flexion assistance should be performed within an entire joint power period rather than just in the negative power phase.

It can be seen from Figs. 10 and 11 that complex responses of the muscles associated have been shown with the exoskeleton application when the human's active movement is hindered. The RF and VM's EMG in ZF mode increase significantly in 15%-25% and 70%-80% of the gait phase, respectively. On the one hand, the overall exoskeleton mass is still borne by the human, which inevitably increases muscle activity. On the other hand, the experimental results demonstrate that additional antagonistic muscle is activated to overcome the disturbance force generated by the exoskeleton.

The predicted joint angle can be used to improve the transparency of the exoskeleton. The appropriate predicted time can be obtained by debugging under constant force command. According to Fig. 12, the experimental results show that the EAO controller designed in this paper can effectively reduce the disturbance force by more than 50%, thereby reducing the antagonistic muscle's additional activation.

Compared to NW, the AP mode decreases the mean EMG of VM, SEM and BF by 25.9%, 6.1% and 7.5%, respectively.

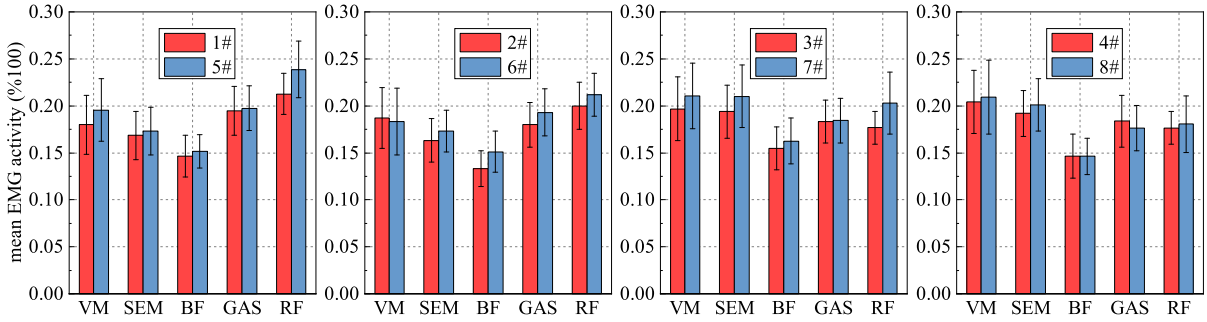

Fig. 8. Muscle activities under designed eight assistance profiles.

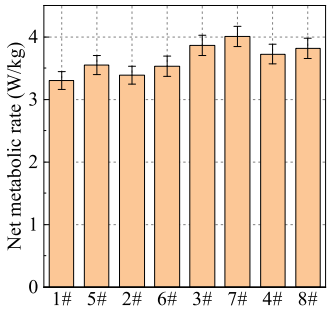

Fig. 9. Net metabolic rate under designed eight assistance profiles.

In terms of peak EMG, the muscles with a decrease are VM, SEM and GAS, which are reduced by 27.6%, 7.2% and 12.4%, respectively. The experimental results demonstrate that assisting at terminal swing and initial contact can reduce muscle activities.

Muscle activities of VM, BF, and SEM at terminal stance remain almost low in both AP and NW modes, suggesting that these muscles' energy storage and return mechanisms are not disturbed. The AP mode decreases the peak EMG of GAS by 12.4% compared with NW. In terms of mean EMG, muscle effort of GAS only decreases by 2.5%, which does not drop as much as peak EMG. In addition, the activation of RF also significantly increases. Correspondingly, the metabolism in AP mode decreases only by 1.3%. Therefore, a metabolic comparison experiment is added to verify whether assistance at the terminal stance is effective. It can be seen from Fig. 13 that the metabolism decreases by 2.7% when assisting the knee joint only at terminal swing and initial contact (APTI).

In Fig. 14, the maximum gait percentages obtained based on the traditional method range from 80.7% to 112.4%, seriously affecting the assistance profile. The method based on EAO significantly improves the accuracy of gait phase division, thereby ensuring the integrity of the assistance profile. The initial value of the fundamental frequency $\omega(0)$ corresponds to the first peak in Fig. 15. The fundamental frequency increases continuously with the increase in walking speed. The experimental results in Fig. 16 can verify that the EAO method proposed in this paper can effectively improve the convergence speed of AO at different walking speeds. According to Fig. 17, the convergence time of EAO is shortened from 200 s to 15 s at speeds of 4.5km/h. The assistance profile designed in this paper is shown in Fig. 18. The reduction in surface contact stiffness also results in lower force-tracking performance at 80%-90% gait phase compared to previous studies. On the whole, the tracking effect can meet the assistance accuracy requirements.

V. Discussion

This study investigates the effectiveness of the CE-based knee flexion-assisted method throughout the gait from the perspective of natural human actuation. On the one hand, we demonstrate that assisting within an entire joint power period and ensuring the human's active movement are prerequisites for the CE-based knee flexion-assisted method. On the other hand, the proposed DFT and FSM can significantly shorten the convergence time and enhance the stability and practicality of EAO in the human-exoskeleton system.

A. Assisting Within an Entire Joint Power Period

The effective energy storage and release mechanism of PE is the key factor for the high energy utilization of the knee joint, which is also one of the distinctive features that distinguish it from the ankle and hip joints. When flexion assistance is performed during the negative work phase, the energy stored in PE decreases as muscle activation decreases. During the positive work phase, the energy stored in PE is released again with the contraction of CE. The energy storage and release mechanism of PE is a chain reaction after the action of CE. The experiments in this paper prove that the shape of the assisting profile should be planned within an entire power period for the knee joint that involves energy storage and release. For other joints, the assistance method proposed in this paper can also be referred to as long as the power of a complete assistance phase includes both negative and positive work.

B. Human Active Movement

Exoskeleton assistance requires higher human-exoskeleton coordination. In other words, if the exoskeleton cannot predict the human motion intention in advance, the disturbance force will be generated due to the system delay during knee extension. At the same time, the activity of the antagonistic muscle has to be forced to increase to counteract the negative work produced by the disturbance force. The assistance effect is attenuated due to the presence of disturbance force. The best prediction time can be obtained by debugging and observing the minimum disturbance force under the constant force command. The EAO controller designed in this paper

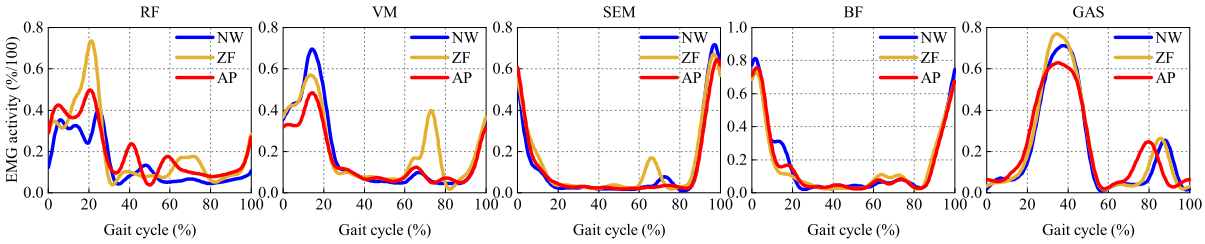

Fig. 10. Average muscle activities of all participants in NW, ZF and AP mode.

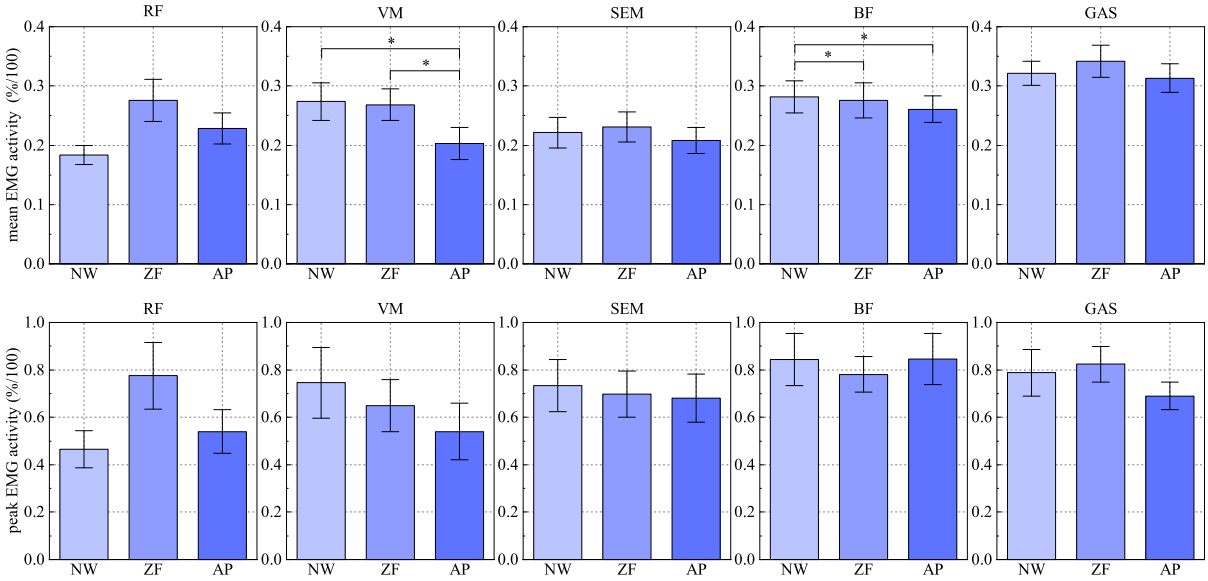

Fig. 11. Mean and peak EMG activities in NW, ZF and AP mode.

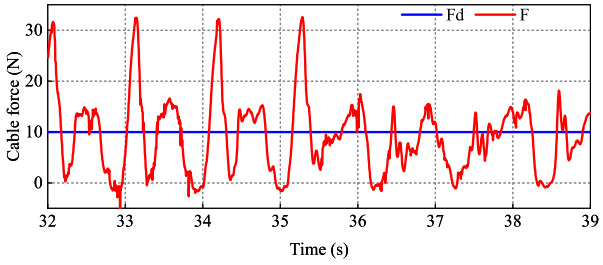

Fig. 12. Dynamic curve under constant force command.

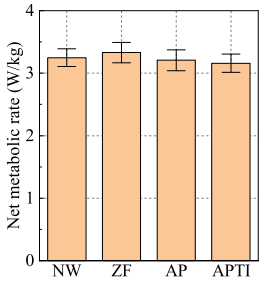

Fig. 13. Net metabolic rate in NW, ZF and AP mode.

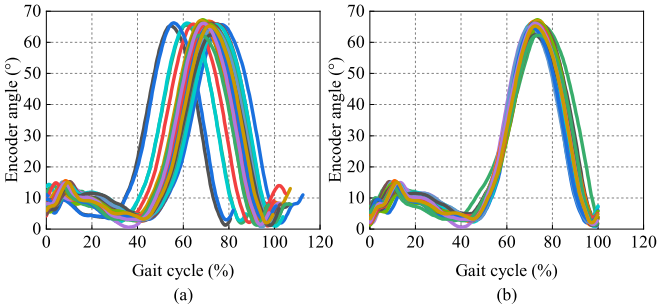

Fig. 14. The gait segmentation curves. (a) with the traditional method. (b) with EAO.

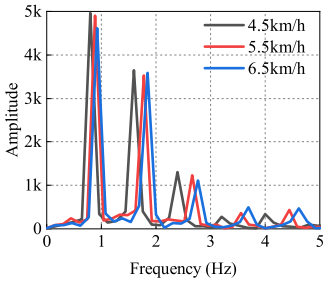

Fig. 15. The frequency distribution obtained by DFT.

can effectively reduce the disturbance force by more than 50%, thereby reducing the antagonistic muscle's additional activation.

C. CE-Based Knee Flexion-Assisted Method

The effect of exoskeleton assistance depends on the assistance profile and the accuracy of force tracking. The net moment of the knee is jointly provided by the exoskeleton, CE and PE. Energy is mainly consumed by CE. Therefore, the preliminary assistance profile in this paper is obtained by subtracting PE from the net biological moment. Complex responses of the muscles have been shown with the

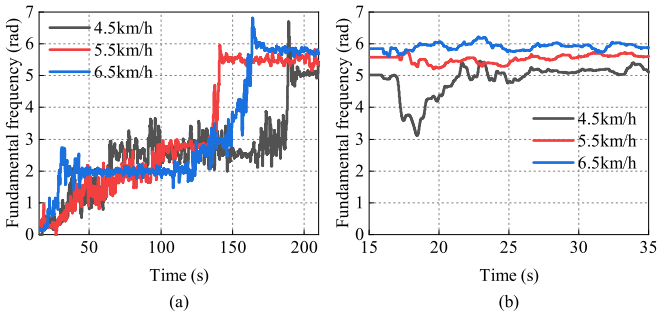

Fig. 16. The fundamental frequency curves. (a) with AO. (b) with EAO.

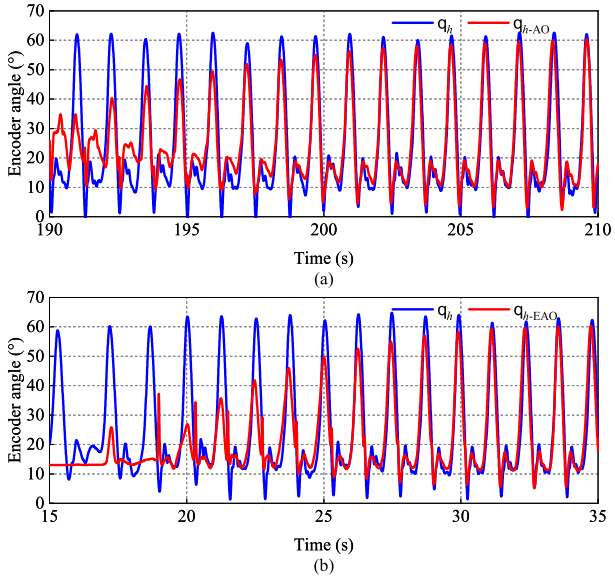

Fig. 17. Learning process for predicting signals. (a) with AO. (b) with EAO.

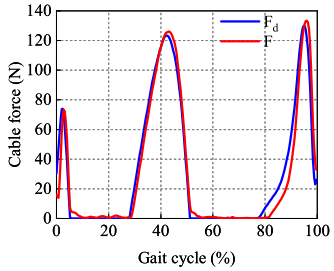

Fig. 18. Dynamic curve under designed assistance profile.

exoskeleton application. The experimental results showed that, except for RF, the activation of the other four muscles decreased with assistance. Interestingly, the reduction in activation is more pronounced in mono-articular muscles than in bi-articular muscles. Previous studies [35] have shown that when hamstring fibers exceed the optimal length, more muscle fibers need to be recruited, which also requires more energy. The optimal fiber length will be longer as the muscle activation decreases, which means fewer muscle fibers are required to output the same muscle force. Further, the corresponding energy consumption will be less. VM's EMG curve also proves the correctness of the above analysis. At terminal stance, all muscles except the GAS maintain a low activation. Moreover, VM, BF, and SEM's muscle activities in AP are almost identical to those in NW, indicating that the energy-returning mechanisms of all three muscles are not disturbed. The GAS transfers energy distally by absorbing energy at the knee during mid to TS, and then returning that energy at both the knee and ankle during the pre- and initial swing. During the negative work, the energy absorption of PE related to GAS is reduced with the decrease of pEMG. When the energy is transferred, ankle assistance should be added to ensure the energy balance. Obviously, it cannot be achieved for single knee assistance. Finally, the energy consumption comparison demonstrates that assisting only at terminal swing and initial contact is optimal.

D. EAO

The requirements for the accuracy of gait phase estimation are higher for the knee joint. The gait percentage obtained based on traditional methods [25] is not always 0-100%, which will seriously affect the assistance profile. In this paper, the motion signal's phase feature is extracted based on EAO. The results show that the gait can be accurately segmented using the phase characteristics of EAO. The disturbance force is reduced by more than 50% with EAO, significantly reducing the corresponding antagonistic muscle activity. Moreover, the DFT-based fundamental frequency estimation method proposed in this paper significantly improves the convergence speed of EAO. The control framework based on FSM also improves the practicality of EAO.

E. Limitations

This study has some limitations. First, we adopt a simplified model to facilitate the analysis of the prerequisite of flexion assistance. More detailed quantitative analysis is still required. Second, the EAO proposed in this paper needs to be further optimized when the movement pattern changes frequently. Third, as we tested, we only performed gait phase estimates, force responses and EMG signals. Although the results indicate some insights, further analyses are still needed.

VI. Conclusion

This study provides insights into the effectiveness of the CE-based knee flexion-assisted method throughout the gait. Specifically, assisting within an entire joint power period and ensuring the human's active movement are not disturbed is a prerequisite for effective flexion assistance based on CE. Moreover, assisting only at terminal swing and initial contact is optimal. We then design the enhanced adaptive oscillator (EAO) to ensure the human's active movement and the integrity of the assistance profile within each gait cycle. The experimental results show that the angle prediction based on the EAO can reduce disturbance force by more than 50%, thereby reducing antagonistic muscle activation. The DFT and FSM are proposed to shorten the convergence time and enhance the stability and practicality of EAO, respectively. The analysis and experiment highlight the importance of designing assistive methods from the perspective of natural human actuation. The mechanism we reveal would also aid the further design of the knee or multi-joint exoskeletons. In future work, we will further perform human-in-the-loop optimization research based on the conclusions of this paper.

REFERENCES

[1] S. Zhang, X. Guan, J. Ye, G. Chen, Z. Zhang, and Y. Leng, "Gait deviation correction method for gait rehabilitation with a lower limb exoskeleton robot," *IEEE Trans. Med. Robot. Bionics*, vol. 4, no. 3, pp. 754–763, Aug. 2022.

[2] T. Huang et al., "Modeling and stiffness-based continuous torque control of lightweight quasi-direct-drive knee exoskeletons for versatile walking assistance," *IEEE Trans. Robot.*, vol. 38, no. 3, pp. 1442–1459, Jun. 2022.

[3] K. Wang et al., "Bio-inspired water-driven electricity generators: From fundamental mechanisms to practical applications," *Nano Res. Energy*, vol. 2, Mar. 2023, Art. no. e9120042.

[4] J. Yan et al., "Recent progress in carbon-based electrochemical catalysts: From structure design to potential applications," *Nano Res. Energy*, vol. 2, no. 2, Jun. 2023, Art. no. e9120047.

[5] M. Khamar and M. Edrisi, "Designing a backstepping sliding mode controller for an assistant human knee exoskeleton based on nonlinear disturbance observer," *Mechatronics*, vol. 54, pp. 121–132, Oct. 2018.

[6] L. Liu et al., "Low impedance-guaranteed gain-scheduled GESO for torque-controlled VSA with application of exoskeleton-assisted sit-to-stand," *IEEE/ASME Trans. Mechatronics*, vol. 26, no. 4, pp. 2080–2091, Aug. 2021.

[7] J. Sun et al., "Realizing self-powered mechanical transmission control system via triboelectric nanogenerator and electrorheological fluid composed soft starter," *Nano Res. Energy*, vol. 2, Sep. 2023, Art. no. e9120066.

[8] K. Knaepen, P. Beyl, S. Duerinck, F. Hagman, D. Lefeber, and R. Meeusen, "Human–robot interaction: Kinematics and muscle activity inside a powered compliant knee exoskeleton," *IEEE Trans. Neural Syst. Rehabil. Eng.*, vol. 22, no. 6, pp. 1128–1137, Nov. 2014.

[9] D. Wang, K. Lee, J. Guo, and C. Yang, "Adaptive knee joint exoskeleton based on biological geometries," *IEEE/ASME Trans. Mechatronics*, vol. 19, no. 4, pp. 1268–1278, Aug. 2014.

[10] Z. Zhang, C. Lung, X. Wei, M. Chen, S. Chatterjee, and Z. Zhang, "In-network caching for ICN-based IoT (ICN-IoT): A comprehensive survey," *IEEE Internet Things J.*, early access, May 9, 2023, doi: 10.1109/JIOT.2023.3274653.

[11] B. T. Quinlivan et al., "Assistance magnitude versus metabolic cost reductions for a tethered multiarticular soft exosuit," *Sci. Robot.*, vol. 2, no. 2, Jan. 2017, Art. no. eaah4416.

[12] H. D. Yang, M. Cooper, A. Eckert-Erdheim, D. Orzel, and C. J. Walsh, "A soft exosuit assisting hip abduction for knee adduction moment reduction during walking," *IEEE Robot. Autom. Lett.*, vol. 7, no. 3, pp. 7439–7446, Jul. 2022.

[13] H. Aftabi, R. Nasiri, and M. N. Ahmadabadi, "Simulation-based biomechanical assessment of unpowered exoskeletons for running," *Sci. Rep.*, vol. 11, no. 1, pp. 1–12, Jun. 2021.

[14] J. J. Kutch and F. J. Valero-Cuevas, "Muscle redundancy does not imply robustness to muscle dysfunction," *J. Biomechanics*, vol. 44, no. 7, pp. 1264–1270, Apr. 2011.

[15] M. Silva et al., "Current perspectives on the biomechanical modelling of the human lower limb: A systematic review," *Arch. Comput. Methods Eng.*, vol. 28, no. 2, pp. 601–636, Mar. 2021.

[16] M. Chen, L. Zhao, J. Chen, X. Wei, and M. Guizani, "Modal-aware resource allocation for cross-modal collaborative communication in IIoT," *IEEE Internet Things J.*, early access, Mar. 31, 2023, doi: 10.1109/JIOT.2023.3263687.

[17] G. Durandau, W. F. Rampeltshammer, H. van der Kooij, and M. Sartori, "Neuromechanical model-based adaptive control of bilateral ankle exoskeletons: Biological joint torque and electromyogram reduction across walking conditions," *IEEE Trans. Robot.*, vol. 38, no. 3, pp. 1380–1394, Jun. 2022.

[18] Y. Zhu, Q. Wu, B. Chen, and Z. Zhao, "Design and voluntary control of variable stiffness exoskeleton based on sEMG driven model," *IEEE Robot. Autom. Lett.*, vol. 7, no. 2, pp. 5787–5794, Apr. 2022.

[19] L. Wang et al., "Resource allocation for multi-traffics in cross-modal communications," *IEEE Trans. Netw. Service Manag.*, vol. 20, no. 1, pp. 60–72, Mar. 2023.

[20] J. R. Koller, C. David Remy, and D. P. Ferris, "Comparing neural control and mechanically intrinsic control of powered ankle exoskeletons," in *Proc. Int. Conf. Rehabil. Robot. (ICORR)*, Jul. 2017, pp. 294–299.

[21] D. Lee, B. McLain, I. Kang, and A. Young, "Biomechanical comparison of assistance strategies using a bilateral robotic knee exoskeleton," *IEEE Trans. Biomed. Eng.*, vol. 68, no. 9, pp. 2870–2879, Sep. 2021.

[22] A. T. Asbeck, S. M. M. De Rossi, I. Galiana, Y. Ding, and C. J. Walsh, "Stronger, smarter, softer: Next-generation wearable robots," *IEEE Robot. Autom. Mag.*, vol. 21, no. 4, pp. 22–33, Dec. 2014.

[23] H. Lu, C. Jin, X. Helu, X. Du, M. Guizani, and Z. Tian, "DeepAutoD: Research on distributed machine learning oriented scalable mobile communication security unpacking system," *IEEE Trans. Netw. Sci. Eng.*, vol. 9, no. 4, pp. 2052–2065, Jul. 2022.

[24] J. Zhang et al., "Human-in-the-loop optimization of exoskeleton assistance during walking," *Science*, vol. 356, no. 6344, pp. 1280–1284, Jun. 2017.

[25] Y. Ding, I. Galiana, C. Siviy, F. A. Panizzolo, and C. Walsh, "IMU-based iterative control for hip extension assistance with a soft exosuit," in *Proc. IEEE Int. Conf. Robot. Autom. (ICRA)*, May 2016, pp. 3501–3508.

[26] C. Livolsi, R. Conti, F. Giovacchini, N. Vitiello, and S. Crea, "A novel wavelet-based gait segmentation method for a portable hip exoskeleton," *IEEE Trans. Robot.*, vol. 38, no. 3, pp. 1503–1517, Jun. 2022.

[27] S. Qiu, W. Guo, F. Zha, J. Deng, and X. Wang, "Exoskeleton active walking assistance control framework based on frequency adaptive dynamics movement primitives," *Frontiers Neurorobotics*, vol. 15, May 2021, Art. no. 672582.

[28] S. Fukashiro, D. C. Hay, and A. Nagano, "Biomechanical behavior of muscle-tendon complex during dynamic human movements," *J. Appl. Biomech.*, vol. 22, no. 2, pp. 131–147, May 2006.

[29] D. L. Morgan, U. Proske, and D. Warren, "Measurements of muscle stiffness and the mechanism of elastic storage of energy in hopping kangaroos," *J. Physiol.*, vol. 282, no. 1, pp. 253–261, Sep. 1978.

[30] N. Hu, Z. Tian, H. Lu, X. Du, and M. Guizani, "A multiple-kernel clustering based intrusion detection scheme for 5G and IoT networks," *Int. J. Mach. Learn. Cybern.*, vol. 12, pp. 1–16, Jan. 2021.

[31] B. Whittington, A. Silder, B. Heiderscheit, and D. G. Thelen, "The contribution of passive-elastic mechanisms to lower extremity joint kinetics during human walking," *Gait Posture*, vol. 27, no. 4, pp. 628–634, May 2008.

[32] R. Kram and C. R. Taylor, "Energetics of running: A new perspective," *Nature*, vol. 346, no. 6281, pp. 265–267, Jul. 1990.

[33] C. R. Taylor, "Relating mechanics and energetics during exercise," *Adv. Vet. Sci. Comparative Med.*, vol. 38A, pp. 181–215, Jan. 1994.

[34] L. Peñailillo, A. J. Blazevich, and K. Nosaka, "Factors contributing to lower metabolic demand of eccentric compared with concentric cycling," *J. Appl. Physiol.*, vol. 123, no. 4, pp. 884–893, Oct. 2017.

[35] M. Shepertycky, S. Burton, A. Dickson, Y.-F. Liu, and Q. Li, "Removing energy with an exoskeleton reduces the metabolic cost of walking," *Science*, vol. 372, no. 6545, pp. 957–960, May 2021.

[36] P. D. Hoang, R. B. Gorman, G. Todd, S. C. Gandevia, and R. D. Herbert, "A new method for measuring passive length–tension properties of human gastrocnemius muscle in vivo," *J. Biomechanics*, vol. 38, no. 6, pp. 1333–1341, Jun. 2005.

[37] Z. Gu, W. Hu, C. Zhang, H. Lu, L. Yin, and L. Wang, "Gradient shielding: Towards understanding vulnerability of deep neural networks," *IEEE Trans. Netw. Sci. Eng.*, vol. 8, no. 2, pp. 921–932, Apr. 2021.

[38] Z. Wang et al., "Study on the control method of knee joint human–exoskeleton interactive system," *Sensors*, vol. 22, no. 3, p. 1040, Jan. 2022.

[39] C. Fleischer and G. Hommel, "A human–exoskeleton interface utilizing electromyography," *IEEE Trans. Robot.*, vol. 24, no. 4, pp. 872–882, Aug. 2008.

[40] T. Lencioni, I. Carpinella, M. Rabuffetti, A. Marzegan, and M. Ferrarin, "Human kinematic, kinetic and EMG data during different walking and stair ascending and descending tasks," *Sci. Data*, vol. 6, no. 1, pp. 1–10, Dec. 2019.

[41] H. Han et al., "Selection of muscle-activity-based cost function in human-in-the-loop optimization of multi-gait ankle exoskeleton assistance," *IEEE Trans. Neural Syst. Rehabil. Eng.*, vol. 29, pp. 944–952, 2021.

[42] Y. Ding et al., "Effect of timing of hip extension assistance during loaded walking with a soft exosuit," *J. Neuroeng. Rehabil.*, vol. 13, no. 1, pp. 1–10, Dec. 2016.

[43] T. Zhou, C. Xiong, J. Zhang, W. Chen, and X. Huang, "Regulating metabolic energy among joints during human walking using a multiarticular unpowered exoskeleton," *IEEE Trans. Neural Syst. Rehabil. Eng.*, vol. 29, pp. 662–672, Mar. 2021.